2DT CONICAL WAVELET WITH HIGH APERTURE-SELECTIVITY FOR DIRECTIONAL SPEED CAPTURE IN VIDEO SEQUENCES

P. Brault, IEEE Senior Member

LSS,
CNRS - Supelec - Paris-Sud University
Gif sur Yvette, France

J-P. Antoine

Inst. Rech. Math. Phys. (IRMP)
UCL, Louvain-la-Neuve, Belgium

ABSTRACT

Cauchy and conical wavelets have been constructed as a response to the lack of aperture selectivity of the Morlet wavelet [1, 2]. Furthermore, they allow a very simple adjustment of their angular selectivity. On the other hand, the Morlet wavelet has been tuned to speed in the 90s [7] and its efficiency has been demonstrated for psychovisual analysis. It has also been used in a powerful aerial target tracking algorithm in [10]. These two interesting developments have been used here to build a new, highly directional, speed-tuned wavelet called Gaussian-conical Morlet (GCM). Like the Morlet wavelet, it presents very good characteristics in motion estimation and tracking, namely, long temporal dependence, robustness to noise and to occlusions. But for aperture selectivity and directional speed-capture, GCM easily outperforms Morlet. This paper describes the GCM construction, utilization and aperture performances.

Index terms — Extraction of motion parameters, continuous wavelet transform, directional wavelets, Morlet, Cauchy and conical wavelets, speed tuning, angular and aperture selectivity, sequence analysis, scalability, optical flow, block matching, sequence retrieval, 2D/3D+T coding, scalable video coding.

1. INTRODUCTION

The continuous wavelet transform has proved to be a very efficient tool for signal analysis. In the late 80s and the 90s, developments to adapt the wavelet transform to various motions have been proposed by Duval-Destin and Murenzi [7, 2]. The group of analysis parameters, i.e., usually position, scale and rotation, has been extended to speed, acceleration and deformation. This has led to various types of time dependent wavelets [2, Chap. 10]. Then a very performant algorithm for missile tracking was set up using such wavelets [10, 2]. In [8, 11] the authors use the same energy-density based algorithm but with, respectively, Expectation-Maximization plus Gaussian mixture approach and scale functional relation plus spatio-temporal (ST) processing blocks.

Later the second authors also use image transformation to time-varying (1D+T) signals. The advantage of velocity detection with the motion-tuned spatio-temporal continuous wavelet transform (CWT) over other known methods, like optical flow (OF) [3], and even block-matching (BM), has been already discussed in [4, 5]. OF and BM work on the motion of pixels or of blocks, but not on regions or objects. They are not inherently scalable either. Like BM, OF has a short time dependence which is not very accurate for slow motion or trajectory estimation. The three characteristics of long temporal dependence, robustness to noise and to occlusions, are the strength of wavelet analysis, and we plan to show it further for pertinent extraction and recognition parameters in sequence analysis, compression and video data mining. Because of its compactness both in position space and in frequency space, the Morlet wavelet was chosen to be tuned to speed, thus giving rise to the Morlet $2D + T$ separable wavelet or DDM (Duval-Destin Murenzi) wavelet. In Fourier space, this wavelet reads as

$$\widehat{\psi}_M(\vec{k}) = \sqrt{\epsilon}\, \exp(-\tfrac{1}{2}|A^{-1}(\vec{k} - \vec{k}_o)|^2) + \text{corr.}, \quad (1)$$

where $A = \text{diag}[1, \epsilon^{-1/2}], \epsilon \geqslant 1$, and the correction term is usually dropped (see [2, Eq.(3.18)]). Nevertheless numerous difficulties remain when using this wavelet in directional analysis. Although it has a good capability for directional filtering, its angular selectivity is poor. It is directional in the sense defined in [1] and [2, Sec.3.3], namely, *"A wavelet ψ is said to be directional if the effective support of its Fourier transform $\widehat{\psi}$ is contained in a convex cone in spatial frequency space"*, but the anisotropy parameter $\epsilon > 1$ is needed in order to get a decent angular selectivity. In addition, the Morlet wavelet has a major drawback: its angular selectivity increases with the length of the wave vector k_0, since the support cone gets narrower, but at the same time the amplitude decreases as $\exp(-|\vec{k_0}|^2)$. On the other hand, conical and Cauchy wavelets are genuine directional wavelets and they don't suffer from that defect. We have used these wavelets as a basis for a new construction of motion-tuned, and in particular speed-tuned wavelets. The development of these wavelets and their use in motion analysis is the aim of the present paper.

2. THE NEW MOTION-TUNED CONICAL WAVELET

2.1. The 2D Cauchy wavelet

The 2D Cauchy wavelet is a prototype of *conical* wavelet, which satisfies the definition of directional wavelet in a strict sense, since its support is a convex cone $\mathcal{C}$ with apex at the origin [2]. It is given in Fourier space by

$$\widehat{\psi}_{l,m}^{\mathcal{C}(-\alpha,\alpha)}(\vec{k}) = \begin{cases} (\vec{k}\cdot\vec{e}_{\widetilde{\alpha}})^l(\vec{k}\cdot\vec{e}_{-\widetilde{\alpha}})^m e^{-\vec{k}.\vec{\eta}}, \text{ for } \vec{k}\in\mathcal{C}, \\ 0, \text{ otherwise,} \end{cases} \tag{2}$$

with α the cone aperture, $\widetilde{\alpha}$ the aperture of the dual cone, $\vec{e}_{\widetilde{\alpha}} \equiv \vec{e}(\cos\widetilde{\alpha}, \sin\widetilde{\alpha})$, $\vec{k}\in\mathcal{C}(-\alpha,\alpha)$, l, m the moments and $\vec{\eta}\in\mathcal{C}(-\alpha,\alpha)$ the cone axis. One usually uses the symmetric version of the wavelet, i.e., with $l = m$, and the axis $\vec{\eta}$ along k_x.

2.2. The 2D Gaussian-conical wavelet (GC)

By definition, the 2D Cauchy wavelet has the property that its opening angle α is *totally controllable* [2], independently of the amplitude, thus it avoids the drawback of Morlet mentioned above. Nevertheless, although it has a good *angular selectivity*, its *radial selectivity* is poor because the exponential term decays slowly as $|\vec{k}| \to \infty$. This is why this exponential is often replaced by a Gaussian along k_x, which concentrates the wavelet on its central frequency $(\sqrt{l+m}, 0)$ [9]. Then $\sigma > 0$ controls the scale localization of the Gaussian. A *center correction term*, $\chi(\sigma) = \sqrt{l+m}\frac{\sigma-1}{\sigma}$, controls the radial support of ψ. This gives the expression of the GC wavelet, in frequency space [2, Eq.(3.37)]:

$$\widehat{\psi}_c^{GC}(\vec{k}) = \begin{cases} (\vec{k}\cdot\vec{e}_{-\widetilde{\alpha}})^m(\vec{k}\cdot\vec{e}_{\widetilde{\alpha}})^m e^{-\frac{\sigma}{2}(k_x-\chi(\sigma))^2}, \ \vec{k}\in\mathcal{C}, \\ 0, \text{ otherwise.} \end{cases} \tag{3}$$

The GC wavelet is shown in Fig. 1.

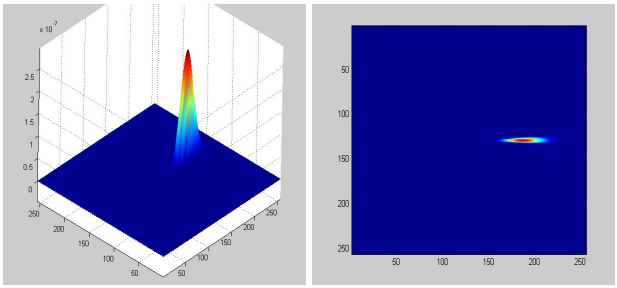

Fig. 1. The 2D Gaussian Conical filter in the (k_x, k_y) plane: the "shark" wavelet; side and top views.

2.3. Construction of the (new) spatio-temporal GCM

Building a wavelet for directional velocity analysis, in a sequence of images, starts by building a spatio-temporal 2D+T wavelet.

Because the 2D Gaussian conical filter has good capacities in spatial resolution and orientation, as well as radial selectivity, it has been chosen as the basis for a velocity-tuned wavelet construction. Thus we take this 2D conical term for the spatial 2D term of our 2D+T wavelet. For the time dimension, we made the choice of a Morlet filter. The resulting 2D+T wavelet is constructed in a separable way in Fourier space: the velocity-tuned 2DT filter is simply the product of the 2D Gaussian conical with the 1D Morlet. We call the resulting wavelet "2D+T Gaussian Conical Morlet" (GCM). Thus it is given in Fourier space as:

$$\widehat{\psi}^{GCM}(\vec{k}) = \begin{cases} \underbrace{\widehat{\psi}^{GC}(k_x,k_y)}_{\text{2D Gaussian conical}} \cdot \underbrace{\widehat{\psi}^{M}(\omega)}_{\text{1D Morlet}}, \\ 0, \text{ otherwise,} \end{cases} \tag{4}$$

with $\widehat{\psi}^M(\omega) = e^{-\frac{1}{2}(\omega-\omega_0)^2}$.

2.4. Tuning the GCM wavelet to motions

Several motion operators can be applied to the "mother" wavelet, like scaling D, translation T, rotation R and speed-tuning Λ:

$$\begin{aligned} [\widehat{D}^{a_s,a_t}\,\widehat{\psi}](\vec{k},\omega) &= a_s a_t^{1/2}\widehat{\psi}(a_s\vec{k}, a_t\omega), \\ [\widehat{T}^{\vec{b},\tau}\,\widehat{\psi}](\vec{k},\omega) &= e^{-j(\vec{k}.\vec{b}+\omega\tau)}\widehat{\psi}(\vec{k},\omega), \\ [\widehat{R}^{\theta}\,\widehat{\psi}](\vec{k},\omega) &= \widehat{\psi}(r^{-\theta}\vec{k},\omega), \\ [\widehat{\Lambda}^{c}\,\widehat{\psi}](\vec{k},\omega) &= \widehat{\psi}(c^q\vec{k}, c^{-p}\omega). \end{aligned} \tag{5}$$

with, for the rotation,

$$r^{\theta} = \begin{pmatrix} \cos\theta & -\sin\theta \\ \sin\theta & \cos\theta \end{pmatrix} \tag{6}$$

Like for the speed-tuned Morlet wavelet, the application of the above operators to the GCM wavelet is done separately on either the spatial 2D conical part or the temporal 1D Morlet, depending on the temporal or spatial nature of the transformation. The values of $p = 2/3$ and $q = 1/3$ align the deformation of the space-time domain with speed [7]. After implementation of the transforms defined in (5), we can give the expression of the 2D+T GCM in terms of the group parameters $g = \{a_s, a_t, \theta, c\}$:

$$\hat{\psi}_{GCM}^{\{a_s,a_t,\theta,c\}}(\vec{k},\omega) =$$
$$\begin{cases} a_s^{-1}a_t^{-1/2}(c^q\, a_s\, r^{-\theta}\vec{k}\cdot\vec{e}_{\widetilde{\alpha}})^l(c^q\, a_s r^{-\theta}\vec{k}\cdot\vec{e}_{-\widetilde{\alpha}})^m \\ \quad \times e^{-\frac{\sigma}{2}(a_s c^{+q}k_x-\chi(\sigma))^2}e^{-\frac{1}{2}(c^{-p}a_t\omega-\omega_0)^2}, \ \vec{k}\in\mathcal{C}(-\alpha,\alpha), \\ 0, \text{ otherwise.} \end{cases} \tag{7}$$

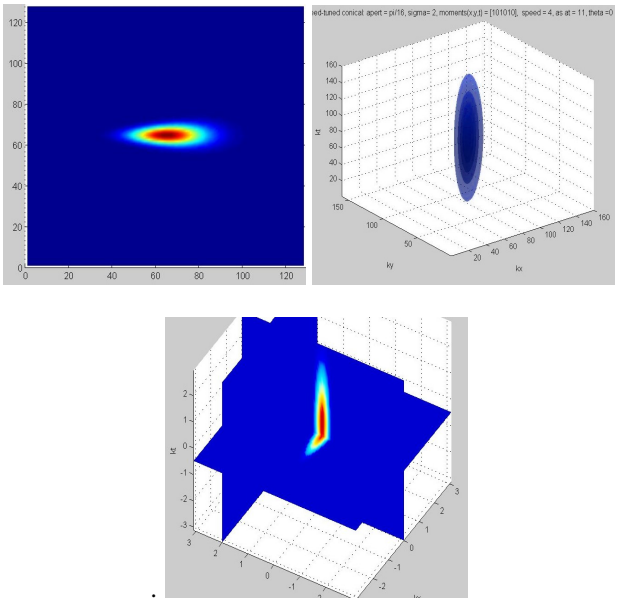

Fig. 2. The 2D+T Gaussian Conical Morlet (GCM) wavelet tuned to speed: (a) Top view in the plane (k_x, k_y) for $c = 1$ and aperture $\alpha = \pi/16$. (b) 3D view in Fourier space (k_x, k_y, ω) for $c = 4$; (c) 3D sectional views in (k_x, k_y, ω) showing the Gaussian amplitude behavior on the (vertical) Morlet part, as well as on the (horizontal) conical part, and for $c = 2$.

The 2D+T GCM wavelet tuned to speed is shown in Fourier space (k_x, k_y, ω) in Fig. 2. From here on, our notation is the following: v_r is the real object speed in the sequence, c the wavelet tuning speed, and v_m the speed measured, on the energy curve, by the speed-tuned wavelet family.

2.5. Speed capture initialization

The GCM wavelet can be transformed to a simple low-pass filter by centering the wavelet in the Fourier plane. This is done by translating the wave-vector $\vec{k}$ of the conical by the value $\vec{k}_0$ (see below) of its central frequency, and by canceling the term ω_0 for Morlet. With this condition, the conical and the Morlet wavelets do not oscillate any more, in fact they are no longer wavelets, but simply filters. They also cannot be tuned to scale. The advantage is that all the "GCM speed-tuned filters" obtained are centered in the Fourier plane and can easily capture the initial speed, due to their shape, independently of the object scale. The initial central wave vector of the conical is $\vec{k}_0 = (\sqrt{l+m}, 0)$. Because it is affected by all the transformations that the wavelet undergoes, we thus compensate the conical wave-vector $\vec{k}$ by the central frequency computed for all transforms, i.e.,

$$\vec{k}_0 = \frac{1}{a_s}\frac{1}{a_t}\frac{\sqrt{l+m}}{c^q}(\cos\theta, \sin\theta) \qquad (8)$$

2.6. Analysis algorithm

For the analysis, we take the product of the whole sequence FFT with each speed-tuned wavelet FFT. An inverse FFT is then applied to the result to give the wavelet transform $\mathcal{W}_\psi(\vec{b}, N, \theta; a_s, a_t, c_j)$ for each speed and for the whole sequence. We then compute the energy density, for each speed, on the basis of a frame or of a group of N_0 frames among the N frames of the sequence. Finally, for the group of speed tunings c_j, we plot the energy, $E_{\rm tot}(c_j)$, of pixels of the selected frames N_0.

$$E_{\rm tot}(c_j) = \sum_{N_0}\sum_{y}\sum_{x} |\mathcal{W}(x, y, N_i, c_j)|^2 \qquad (9)$$

Then we study the curve $f(c_j) = E_{\rm tot}(c_j)$. This curve will go through a maximum, v_m, when the speed of the tuned wavelet c_j matches the real speed v_r of the object (a travelling 2D Gaussian here). Several algorithms could be used to optimize the search for the maximum of the energy. This could be done, for example, by using a dichotomy rather than sweeping the whole range of velocity tunings, or by using Nelder-Mead as in [10].

3. EXPERIMENTATION

We first want to recall the results obtained in speed computation [5] between the Morlet speed-tuned CWT and the OF: Total computation speed (Xeon bi-processor at 2.4gHz):
(1) MTSTWT with 3 wavelets tuned to 3 speeds (3,6,10 pixels/fr) on a $360 \times 240 \times 8$ sequence block (Tennis sequence) at the highest resolution of scale:
$t_{\rm MTSTWT}(1200\text{ms}) + 3 \times \text{IFFT3D}(3 \times 380\text{ms}) = 2.4\text{s}$.
(2) Fast Optical Flow with wavelets [3] between two frames and 4 different resolutions : $t_{\rm OF}$ =10s.

In Fig. 3, we show the orientations that Morlet and GCM can take for $0 \leqslant \theta \leqslant +\pi/2$. This figure speaks by itself. Morlet is shown with only one orientation. The reason is that a variation of its selectivity parameter ϵ results in a displacement along the radial support of the wavelet. This displacement is large enough to see, on the same radius, all the shapes that Morlet takes if we increase the couple (k_0, ϵ). We show four couples $k_0 = \{6, 12, 22, 35\}$ and $\epsilon = \{1, 2, 5, 13\}$. We can see that the angular selectivity is very hard to adjust. For weak values of k_0 and/or ϵ, the aperture is very large. This aperture decreases by increasing k_0 and ϵ. But as k_0 increases, Morlet moves away, from the Fourier center (0,0), on its radius. This makes very difficult the spatial positioning of this wavelet with respect to a change in aperture selectivity. On the contrary, with GCM the couple orientation/aperture is extremely simple to adjust. We show five orientations $\theta = \{0 \text{ to } \pi/2\}$ with GCM tuned to aperture $\alpha = \{\pi/256 \text{ to } \pi/16\}$. This proves the very good aperture selectivity of GCM.

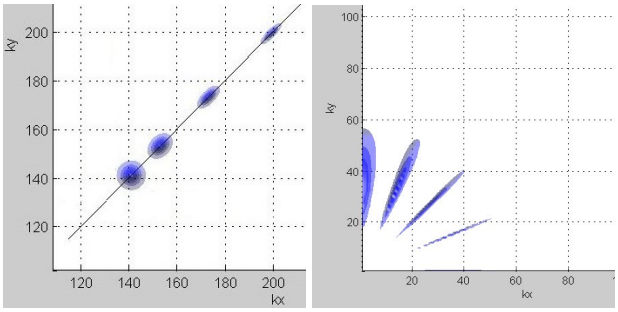

Fig. 3. Comparison of aperture selectivity tuning between Morlet and GCM. The figures show that both wavelets are easily rotated. But, on panel (a), the Morlet wavelet behaviour, w.r.t. a tuning of its selectivity parameter ϵ, is awkward : the wavelet moves on its radius with α and its radial extension is not constant, and limited. On the contrary, panel (b) shows that on GCM, a variation of the aperture does not implies any displacement on its radius, and that the radial extension is constant and easily adjustable. For sake of clarity we show the result for five rotations of GCM ($\theta = 0$ to $\pi/2$).

We now perform a comparison between the 2D+T Morlet and the 2D+T GCM. We use a test sequence of $128 \times 128 \times 32$, that includes the motion, at constant speed, of a 2D non-symmetrical Gaussian. The angles of the Gaussian and of its trajectory are varied (along k_x, at 45° and along k_y).

The first experiments have been done with a symmetrical Gaussian travelling at constant speed in the plane. We checked that speed capture is as good with GCM as with Morlet. But this is not the real interest of this study. We then modified the Gaussian to exhibit a strong anisotropy in the direction OY in the spatial plane. For this we took a large σ_y (i.e., in the OY direction) and a small σ_x. The larger σ_y, the narrower its spectrum along the k_x direction in the Fourier domain. Thus we are able to test the angular, or more exactly, the aperture selectivity of the wavelet, i.e. its accuracy in directional speed capture. The orientation of the object will also be its spectral "signature" and will enable to "capture" it in a sequence and to assign it its speed (Fig. 4).

In the 3D Fig. 4, we can observe the spectrum of the Gaussian, oriented along k_x (OY in the direct space) and of large σ_y, and travelling (along OX in the direct space) at a speed $v_r = 3$ pix/fr. The figure shows the "interception" of the spectrum by the hyperbola-like family of GCM wavelets tuned to speeds between 1 and 6 pixels/fr. The aperture is $\alpha = \pi/16$ and the spatial and temporal scales are $a_s = 3$ and $a_t = 3$. By looking again at Fig. 3, panel (a), it is obvious that in the same conditions, a change of aperture of the Morlet wavelet would result in a displacement of it on its radius, thus in a change of spatial position and scale. The poor angular selectivity of Morlet, together with speed-tuning, thus makes the directional capture of the spectrum very difficult. This does not happen with GCM. This makes it very efficient in capturing the signal speed at any angle within a constant and narrow conical aperture $\alpha = \pi/16$ and not outside it. We will also show further that GCM can achieve much narrower apertures in speed-capture.

In Fig. 5, we plot the curve v_m vs. θ_{wav} for $-\pi/2 \leqslant \theta \leqslant +\pi/2$, with GCM. The correct speed is captured when the wavelet orientation ($\theta = 0$) exactly corresponds to the spectrum orientation (k_x). This proves the good angular selectivity of GCM, that could not be reached with Morlet, and its efficiency to detect the correct speed of the sequence in a very narrow angular aperture and not elsewhere.

The final Fig. 6 demonstrates the excellent performance of GCM during a speed capture at $v_r = 4$ and for more and more narrow conical apertures. We have taken apertures of $\pi/8, \pi/16, \pi/64, \pi/256$ (0.70 deg). The capture conditions are those of Fig. 4, where the spectrum, oriented in the k_x direction, is narrow, and for a real speed $v_r = 4$. GCM captures the spectrum for extremely weak apertures without moving in the Fourier space. This makes it very robust to scale initialization and object size detection and tracking, which is one a the major drawbacks of speed capture with Morlet.

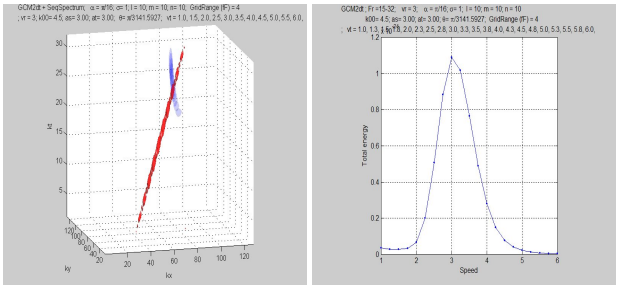

Fig. 4. Demonstration of speed capture in the Fourier domain with $v_r = 3$. (a) The spectrum of the travelling Gaussian intersects the speed-tuned wavelets hyperbola-like family. (b) The energy sum plotted w.r.t wavelet speed tuning (v_t). The maximum is exactly reached for $c = v_r = 3$ pix/fr.

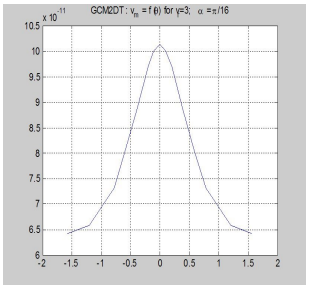

Fig. 5. Result : Performances of GCM in directional speed capture: we plot the curve v_m vs. θ_{wav} for $-\pi/2 \leqslant \theta \leqslant +\pi/2$ for an aperture $\alpha = \pi/16$ and $v_r = 3$. The correct speed is captured when the wavelet orientation ($\theta = 0$) exactly corresponds to the spectrum orientation (k_x).

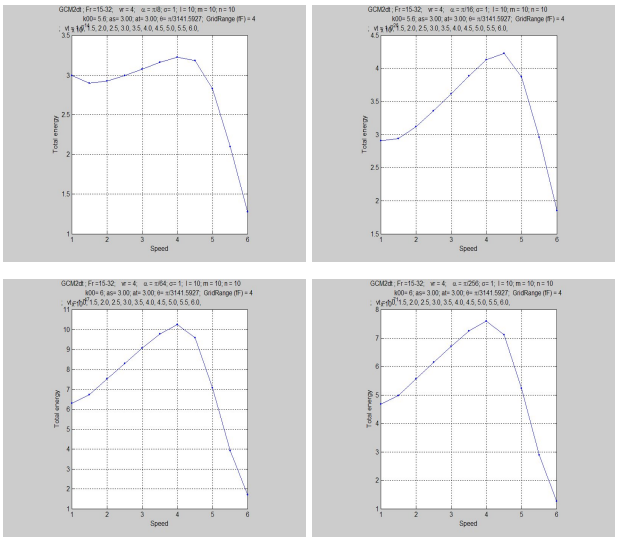

Fig. 6. These 4 figures show the excellent performance of GCM during a speed capture at $vr = 4$ and for more and more narrow conical apertures, respectively : $\pi/8, \pi/16, \pi/64, \pi/256$ (0.70 deg).

4. CONCLUSION

This paper has introduced a new tool, based on the redundant CWT, for directional speed analysis in video sequences, namely, a new speed-tuned wavelet, the Gaussian-conical-Morlet (GCM). It is based on a 2D Cauchy-conical genuine directional wavelet, on one hand, together with a temporal 1D Morlet wavelet, on the other hand, and it provides a very high directionally selective speed-tuned wavelet. This widely improves the characteristics of the 2D+T Morlet wavelet previously used in spatio-temporal speed-based approaches of motion estimation and tracking. It thus reinforces the efficiency of the CWT tool for speed and motion tracking, and in particular its inherent robustness to noise, occlusions and local illumination variations as well as its efficiency to long dependence analysis. In this work we have proved the extreme efficiency of this tool in directional speed selectivity (the aperture of the conical wavelet) down to angle apertures of less than 1 degree ($\pi/256$). An initialization of the speed capture has also been proposed by turning the GCM wavelet to a simple low-pass directional filter centered in the middle of the Fourier plane.

Concerning the application on complex synthesized video sequences with several objects (Gaussian shapes), accelerated motions and occlusions, we refer to the results obtained with DDM wavelets [10], results that can be applied to GCM wavelets that outclass the capacities of DDM wavelets. The test of GCM in real video sequences is planned for a future work and for applications in the domains of selective (through spectral signature) motion estimation, trajectory estimation, motion tracking and feature/sequence retrieval.

5. REFERENCES

[1] J-P. Antoine, R. Murenzi and P. Vandergheynst, Directional wavelets revisited: Cauchy wavelets and symmetry detection in patterns, *Applied Comput. Harmon. Anal.*, 6, pp 314–345, 1999.

[2] J-P. Antoine, R. Murenzi, P. Vandergheynst, and S.T. Ali, *Two Dimensional Wavelets and Their Relatives*, Cambridge University Press, Cambridge (UK), 2004.

[3] C. Bernard, *Ondelettes et problèmes mal posés: la mesure du flot optique et l'interpolation irrégulière*, PhD thesis, Ecole Polytechnique, Palaiseau, Nov. 1999 (English version: `www.cmap.polytechnique.fr/∼bernard/these`)

[4] P. Brault, A new scheme for object-oriented video compression and scene analysis based on motion-tuned spatio-temporal wavelet family and trajectory identification, *IEEE ISSPIT 2003, International Symposium on Signal Processing and Information Technology*, pp 250–254, Darmstadt, Germany, 2003.

[5] P. Brault, *Motion Estimation and Segmentation*, PhD thesis, Paris-Sud University, Nov. 2005.

[6] E.J. Candès and D.L. Donoho, Continuous curvelet transform. I-II. *Appl. Comput. Harmon. Anal.*, 19, pp 162–197; 198–222, 2005.

[7] M. Duval-Destin and R. Murenzi, Spatio-temporal wavelets: Application to the analysis of moving patterns, in *Progress in Wavelet Analysis and Applications (Proc. Toulouse 1992)*, pp 399–408; Y. Meyer and S. Roques (eds.), Ed. Frontières, Gif-sur-Yvette, 1993.

[8] L. Hong, Y. Ruan, W. Li, D. Wicker and J. Layne, Energy-based video tracking using joint target density processing with an application to unmanned aerial vehicle surveillance, *IET Computer Vision*, Vol.2, No 1., pp. 1-12, 2008.

[9] L. Jacques, *Ondelettes, repères et couronne solaire,* PhD thesis, Université Catholique de Louvain (UCL), Louvain-la-Neuve, 2004.

[10] F. Mujica, J-P. Leduc, R. Murenzi, and M.J.T. Smith, A new motion parameter estimation algorithm based on the continuous wavelet transform, *IEEE Trans. Image Process.*, 9, pp 873–888, 2000.

[11] R. Wang, Y. Zhao, Y. Liu and Y. Yuan, A target tracking algorithm based on the continuous wavelet transform of spatio-temporal processing block, *International Conference on Electronics and Optoelectronics (ICEOE)*, Vol.2, pp.95–98, 2011.